

Multi-Methods of Measurements of Cosmic Rays by DIY Geiger counter

Hsiang-Yu Chen¹ and Jin-Tong Feng¹

¹*Department of Physics, National Taiwan University, Taipei 10617, Taiwan*

Instructor: Jiwoo Nam¹

Cosmic rays play a vital role in Astroparticle physics processes. In this paper, we mainly focus on muon measurements. In hardware and software, we build muon detectors in multiple approaches from analog to digital counters. We first use our handmade device to reproduce the results of previous classic experiments, like testing the size distribution of air showers (Auger et al. 1939), checking the East-West effect, etc. Then we conduct two tunnel experiments for measuring part of the column densities of mountain ranges around Taipei. We also discuss air pressure, height - muon counts relations and show similar trends as Victor Hess's work in 1912. For extra application, we operate a radioactive rock test of Torbernite and Hokutolite.

I. INTRODUCTION

Cosmic rays are high-energy particles originating from deep space, their origins ranging from distant galaxies to supernovae within our own Milky Way. The detection and study of cosmic rays have unveiled a wealth of knowledge about the universe and its fundamental processes.

One crucial aspect of cosmic ray research involves understanding how these particles interact with matter as they traverse through it. The **Bethe-Bloch formula** provides a path to calculate the energy loss of charged particles, such as muons, as they pass through a material medium. It describes the energy deposition per unit path length, taking into account factors such as the particle's charge, mass, and velocity, as well as the density and atomic number of the material. The Bethe-Bloch formula has been instrumental in comprehending the energy loss mechanisms and enabling the identification and characterization of cosmic ray particles.

When cosmic rays collide with the Earth's atmosphere, they generate a cascade of secondary particles known as an air shower. These cascades consist of a multitude of particles, including **muons**, which are particularly intriguing due to their penetrating power. Muons possess the unique ability to traverse substantial distances and even penetrate deep into the Earth's surface.

In this project, we design portable muon detector to discuss several properties of muons, including reproducing previous works like Air shower distribution, Zenith angle and East-West effect in Section III-A to C. In section III-D to G, we expand the applications of our device to measure column densities of tunnels, radioactive rock tests and muon flux densities with air pressure & altitude relations.

II. INSTRUMENT

We would like to divide the methods of the project into three main parts: the first part is **Instrument Design**, we design our muon detector in multiple approaches and integrate them. The next part is **Software and Data Analyses**, we come up with MCU with an SD card reader for recording data. The final part are **Cosmic Rays Experiments**, we use our handmade muon detector to operate various kinds of particle experiments, and the explicit explanations of the experiments are shown below.

A. Instrument Design

1. Hardware

Geiger counter, is a kind of instrument for detecting and measuring ionization radiation, such as α particle, β particle, and γ ray. It was first developed by Hans Geiger and Walther Müller in 1928. Geiger-Müller tube, which is the main core of the counter, is filled with inert gases like argon, helium, or neon at low pressure, with high voltage applied. When the cosmic ray signal passes through, the gas in the tube would be ionized by the incident radiation, hence the circuit is briefly conducted. Due to the high voltage and EM-shower causing an "avalanche" in the tube, the small signal pulse could be considerably amplified.

To produce high voltage for operating the Geiger-Müller tube **CI-22G** in our instrument at which range is 360-400 V as a condition of the flat plateau for stable operation, we design the **Analog Signal Module**. Inside the analog board, we use KSP44 Transistor for the voltage amplifier, and Figure 1 shows the result of the amplification of the pulse signal passing through two Geiger-Müller tubes.

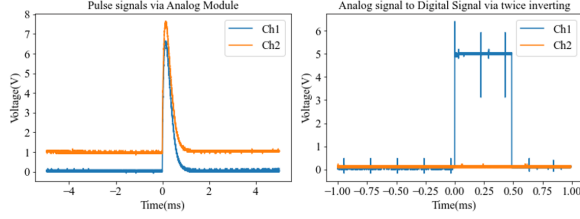


FIG. 1: We translate Ch2 +1V for distinguishing signals from two channels in left figure. The right figure is the digital signal converted by IC 74CH14.

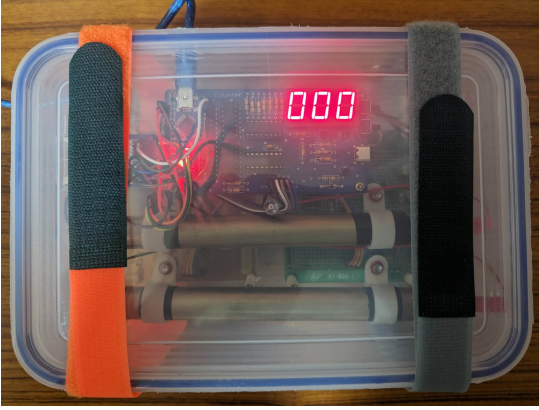


FIG. 2: Our handmade portable muon detector with plastic box covered for enhancing robustness.

For better ways to analyze data, we then build the **Digital Signal Module** to produce digital logic gates when analog inputs from Geiger-Müller tubes are given. This module consists of four parts: the first one is using 74CH14 Hex inverters to issue digital signals upon arriving GM pulses. The second part is a high-pass filter, for eliminating low-frequency ripples; then we use discriminator via Schmitt trigger circuit to eliminate small noise pulses. At last, we also add an LED driver for each channel, to display when pulse signals arrive.

Further, we build **Coincidence and Counter board**. In this section, we use logic gates and filters which issues an output when both inputs are ON, and the three-digit digital counter is to display the output of the coincidence test in the 7-segment display, which allows us to record event numbers. For the convenience of data collection, we add SD card reader module in our circuit to record data in the experiments. We also add the BMP280 module air pressure and temperature sensor, for measuring muon counts with altitude and pressure relations.

2. Software and Data Analyses

To make our record of experiments more efficiently, as well as diversify functionalities of our handmade muon detector, we remain some space for the **micro control unit (MCU)** in the Counter board. we select **Arduino Nano** for its tiny size, intuitive C code basics, and portability. After dealing with the loop delay of Arduino itself, and port manipulation for reading decimal from binary, we successfully record the pulse signals with almost the same counts as the 3-digit counter board shown.

For Data analyses, we deal with uncertainty by setting \sqrt{N} as the standard deviation, where N is the count rate of muons. This method is widely used in scientific analyses.

III. METHODS

So far, we have conducted several experiments like overburden dependence in Old Caoling Tunnel and Xinhai Tunnel, zenith angle dependence, etc. In this section, we will show how we conduct these measurements.

A. Air Shower Distribution

In the air shower size experiment, we want to measure the size of a shower, therefore we modify the distance between two Geiger-Müller tubes and measure the counts. We can estimate the size and the distribution of the shower. The difference between indoor and outdoor can be predicted by the Rossi curve where the indoor one propagates through concrete layers with higher density, hence it's more likely to produce a shower. We conduct the experiments in Room 923 and at the 11 floor balcony of the Astromath building in NTU.

B. Zenith Angle

Supposed that the atmosphere is rotational symmetry, the length which muons propagate with an inclination angle is longer than the length where muons propagate with zero inclination and this means that it's more likely that muons produce showers and turn into other particles. In general, the distribution of intensity as a function of the zenith angle should be like $\cos^2(\theta)$ where θ is defined as the angle between the orientation of the detector and the norm direction of the horizon.

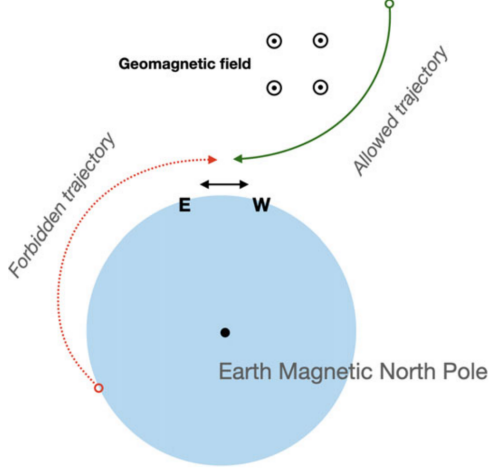


FIG. 3: This figure shows the trajectory of charged cosmic rays in the geomagnetic field. Credit: Neil Ashby et al. (2021).

C. East-West effect

Trajectories of charged particles are curved when they travel through a magnetic field from which the force is given by the Lorentz force. The Lorentz force is

$$q\vec{v} \times \vec{B} = m\frac{v^2}{r} \quad (1)$$

where we assume the velocity and the geomagnetic field are vertical and the geomagnetic field can be seen as a dipole expressed as

$$B = \frac{\mu_0}{4\pi} \frac{P}{r^3} \quad (2)$$

with the geomagnetic momentum P at the equator. The direction of positively and negatively charged particles are opposite. More precisely, we are more likely to detect cosmic rays with a positive charge when we orient our detector to the west and vice versa. In other words, the intensity of positive-charge cosmic rays like protons is greater than the intensity of negative-charge cosmic rays. In this experiment, we want to reproduce the result of Bruno Rossi (1930) who first found the asymmetry. We orient our detector toward the east and west and measure the intensity of cosmic rays.

D. Radioactive Rocks Measurement

Our muon detector uses two Gieger tubes to probe muons. However, we can also use this detector to detect the radiative sources. We measure the emissivity of **Torbernite** and **Hokutolite** borrowed from

Prof. Wen-Shan Chen in the Department of Geoscience. Specifically, we align the detector and rocks such that the high-energy particles can penetrate tubes as coincidence test. It is likely that there are some radiative sources in the building of the Department of Geoscience so measuring the background to prevent the contamination. Both Torbernite and Hokutolite are radiative where Torbernite contains ^{222}Rn , half-life ≈ 3.8 days, and Hokutolite has a small amount of Radium, Polonium, etc.

E. Tunnel Experiment

The Rossi curve predicts that possibility of shower via hadronic scattering increase increases once muons travel in a dense medium. We measure the intensity of muons in the tunnel. If the height of a mountain increases monotonically before the maximum altitude, the deeper we go in the tunnel, the fewer muons we can measure. We perform the experiment both in the Xinhai tunnel and the old Caoling tunnel. The Xinhai tunnel is short, hence we measure muons every 24 or 48 meters. However, the old Caoling tunnel is about 2 kilometers which is much longer than the Xinhai tunnel, we therefore measure muons every 100 meters. Because the scales of the two tunnels are different, by measuring muons we can acquire the effect of buffering in different scales.

F. Height and Cosmic rays

Muons are decelerated and produce shower via hadronic scattering in the air. In the atmosphere, the process is related to the density and depth through which they propagate, so the most direct way to examine this relation is to measure the muon intensity as a function of pressure. However, the atmospheric pressure fluctuation is small to see the effect. The distribution of air in the atmosphere is exponential so the intensity soars as a function of height. We go to Mt. Lulin with a height of 2880 meters roughly. Figure 4 demonstrates our detector at the peak of Mt. Lulin, within a handmade box for enhancing the robustness of our device.

G. Pressure Measurement

The pressure measurement and the height measurement are almost the same. In principle, the atmospherical pressure and intensity are anti-correlation. Atmospherical pressure fluctuates every day so we measure the intensity and the pressure for several days. However, the pressure fluctuation

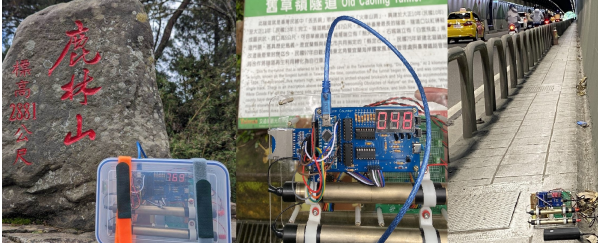


FIG. 4: This figure shows our detector on Mt. Lulin, the old Caoling tunnel, and the Xinhai tunnel.

in Taiwan is too small to observe a significant relation between pressure and intensity. Consequently, we also conduct the pressure measurement at Mt. Lulin (Altitude: 2884 m) for a day to see the relation compared to the fluctuation in Tainan plain.

IV. RESULTS AND DISCUSSION

A. Air Shower Distribution

Figure 6 demonstrates the size of the shower and the intensity decreases as a function of distances quickly, which reveals the spatial distribution of local showers. The intensity of the outdoor experiment is larger than the indoor one insignificantly except for the data with a distance of 20 cm. In general, the intensities of the indoor and outdoor experiments are consistent, which is beyond our expectations. The Rossi curve states that intensity increases when muons propagate through a lead wall and decrease when the lead wall is thick enough. In our experiment, the effect of a lead wall is replaced by concrete layers. We come up with three reasons to explain why the result is inconsistent with our expectations.

1. Room 923 is at the corner of the Astro-math building, and it's possible that not all muons would penetrate the concrete layer. In other words, muons may come from the sides of the building. Under this circumstance, the effect of the concrete may be weakened.
2. We have limited time on the balcony of the Astro-math building due to regulations. Generally, the measurement time of the outdoor experiment is less than the indoor experiment. This means that the outdoor experiment is more vulnerable to outliers. In Pierre Auger (1939), the relation between intensity and distance is linear in the log scale within one meter. Consequently, We can use the linearity of the relation to examine our result. Our result in the log scale is shown in

Figure 5. The upper and lower panel indicate the indoor and outdoor experiments respectively. The regression line for the indoor experiment is $y = (-0.70 \pm 0.09)x + (0.71 \pm 0.27)$ and for the outdoor experiment is $y = (-0.75 \pm 0.19)x + (0.78 \pm 0.55)$. The regression lines are consistent with each other, which indicates the effect is not significant. However, the r^2 are 0.93 and 0.79 for indoor and outdoor experiments respectively. The r^2 values indicate the effect of outliers which is consistent with our expectations. To improve the experiment, we can

1. elongate the measurement time: longer measurement time can reduce the uncertainty and the effect of outliers.
2. conduct the experiment in a large basement such as a parking lot: under this circumstance, all muons travel through the concrete.

B. Zenith Angle

Figure 7 demonstrates the intensity as a function of the zenith angle. The fitting shows that the data and theory are consistent at small zenith angles. The intensity is deviated positively at large zenith angles. The deviation is from the local shower effect, in other words, it degenerates back to the local shower experiment when we put tubes parallel. What we want to measure is only muons along certain directions so the point here is that the $\cos^2(\theta)$ does not consider the effect of local showers. At lower zenith angles, the intensities of muons are high enough that muons dominate over the effect of local showers. However, at large angles where the muons are almost along the direction parallel to the horizon, the intensities of muons are so low that the local shower effect is significant, which leads to a positive deviation. We have two methods to correct the effect of local showers.

1. We can wrap a layer of aluminum foil such that it can block particles such as electrons or photons produced in the shower.
2. We can measure the effective distance, i.e. projected distance, of two tubes and use the relation we find in the local shower size to correct the effect of the local showers.

C. East-West Effect

Figure 8 shows the distribution of the intensity as a function of zenith angles for east and west orientation respectively. The intensity of the west orientation is larger than the east one within 60 degrees

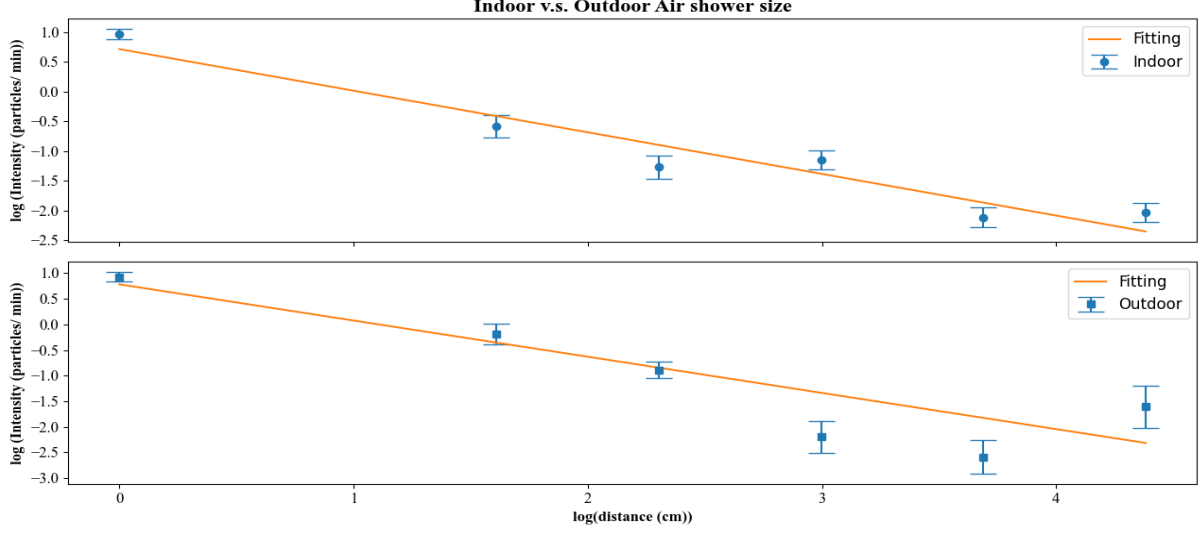


FIG. 5: This figure demonstrates the relation between the intensity and the distance in the log scale.

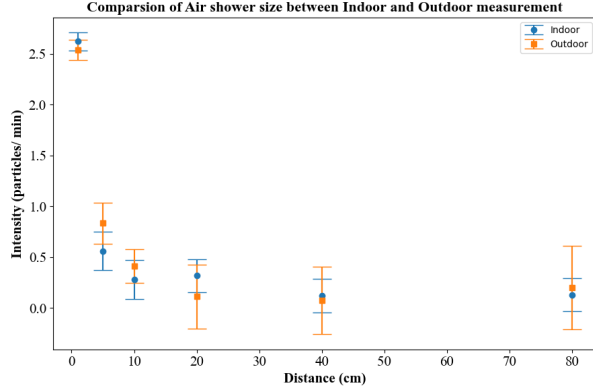


FIG. 6: This figure shows the distribution of intensity as a function of distance.

by roughly one sigma, which is consistent with our expectations. However, both results are consistent with each other when the zenith angle is larger than 70 degrees. The reason is the same as the zenith angle experiment. At larger angles, the effect of the local shower is more dominant over the cosmic rays along the direction parallel to the horizon.

D. Radioactive Rocks Measurement

Figure 9 shows the result of the rocks experiment. The intensity of Torbernite is larger than the background by at least three sigmas, which indicates that it contains a great number of radiative chemical components such as radium. However, the intensity of Hokutolite is larger than the background insignifi-

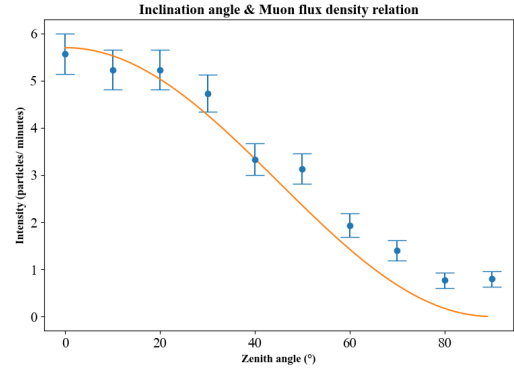


FIG. 7: This figure shows the distribution of intensity as a function of the zenith angle. The blue dots are data from observation and the orange line is the fitting of $\cos^2(\theta)$

cantly, say by one sigma roughly. Kimura, K., (1940) claimed that there are only 1.3×10^{-9} grams radium per gram of Hokutolite. The amount of radiative sources in the Hokutolite is extremely rare so the effect is not significant. Besides, the intensity of rocks is also related to the size of the rock and the ratio of radiative source and non-radiative source in the rock.

E. Tunnel Experiment

We transfer the depth that we go into the tunnel to the column density for two tunnels shown in Figure 10. We find that the intensity declines fast as

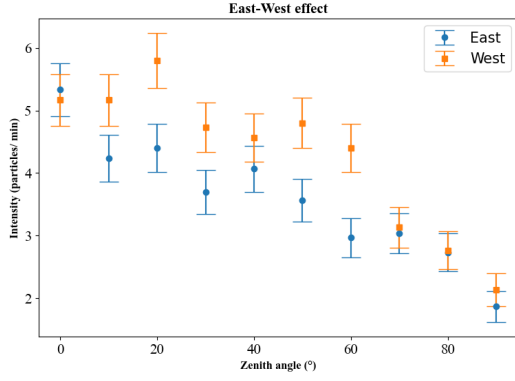


FIG. 8: This figure demonstrates the intensity difference between east and west orientation.

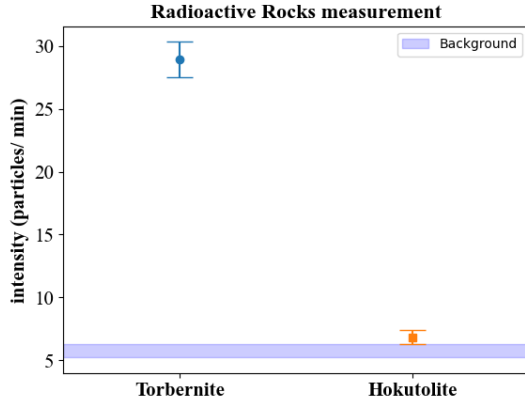


FIG. 9: The figure demonstrates the intensity of high-energy particles emitted by Torbernite and Hokutolite where the blue shaded area is the background value with one sigma uncertainty.

a function of the rock column density, which is consistent with expectations. Noted that the last data point of the Xinhai tunnel is significantly higher, we consider that it may be just a statistical outlier or there are some short-circuit caused by the collision during transportation. Besides, The most mysterious event in the old Caoling tunnel was that channel two could not measure anything even though we changed the orientation and the zenith angle when we measured muons in the tunnel meanwhile channel one kept blinking. We left the tunnel and examined the detector and changed the port of the battery but the problem was not alleviated. We suspect that this is likely triggered by the collision during transportation. Consequently, we only measured muons as a function of depth several times only when channel two worked properly, i.e. channel one and channel

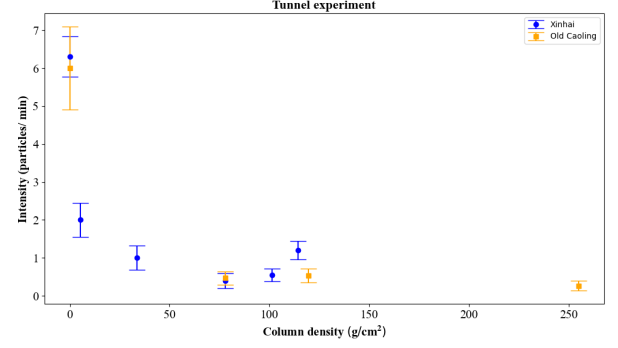


FIG. 10: This figure shows the intensity as a function of column density.

two blinking with similar frequency, we do measure muons.

F. Height and Cosmic rays

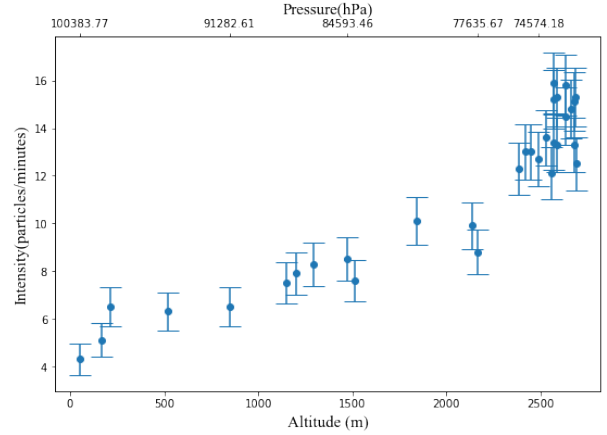


FIG. 11: The figure demonstrates the intensity of muons as a function of atmospheric pressure and altitude

The result is shown in Figure 11. As altitude increases, atmospheric pressure decreases, and the intensity increases, which is consistent with our expectations. Pressure decreasing means that there are fewer air atoms on the path so the intensity of muons soars. It's less likely that muons scatter with hadrons and produce showers. It seems that the relation after 2500 meters is not clear and we regard that it's likely due to the resolution inefficiency. In other words, the height difference is not larger enough to see the trend.

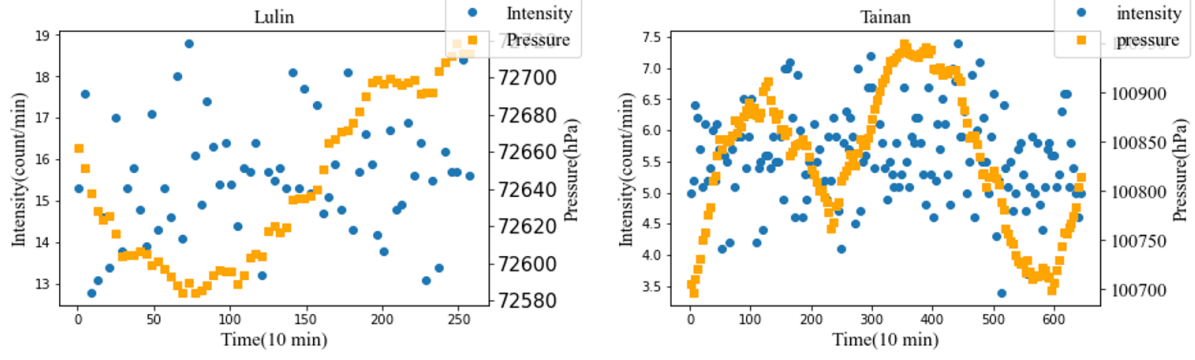


FIG. 12: The figure shows the relation between atmospheric pressure fluctuation and intensity. The left and right plots are for Lulin and Tainan.

G. Pressure Measurement

In the end, we conduct the pressure experiment at Mt. Lulin and Tainan for a day respectively. Figure 12 shows the result. We find the anti-correlation insignificant. We consider that the insignificance is due to small fluctuation and short observation time.

V. CONCLUSION

First, we build a portable muon detector which consists of two Gieger tubes, an analog board, etc. Before assembling everything together, we measure the muon intensity as a function of the distance between two Giger tubes indoors and outdoors. We find the intensity declines quickly at small distances, which reveals the distribution of the local shower. Besides, the results of indoors and outdoors are consistent and we consider that we can observe higher indoor muon intensity if we do the experiment with thicker concrete layers. Then, we measure the muon intensity as a function of the Zenith angle and do the experiment again with east and west orientation. We find the relation between intensity and the Zenith angle is $\cos^2(\theta)$ for small angles which is consistent with the theory. It's likely that the data is contaminated by local showers so the deviation appears at larger angles.

Besides, we borrowed Torbernite and Hokutolite from Prof. Wen-Shan Chen and measured the emissivity of rocks. We found that the emissivity of Torbernite is significantly higher than the background value, which indicates that there are some radiative chemical components in Torbernite. On the other hand, it's not significant for Hokutolite and we regard that it's due to the amount of the radiative components in Hokutolite. To examine the effect of air showers, we can measure the relationship between atmospheric pressure and intensity. Consequently, we go to Mt. Lulin and measure the intensity and pressure as a function of height. In general, the intensity increases as pressure decreases, which is consistent with our expectations.

VI. ACKNOWLEDGEMENT

First, we give sincere thanks to Prof. Nam for hosting this fantastic lecture and giving good guidance also suggestions. Then, we thank Prof. Wen-Shan Chen, a distinguished professor in the Department of Geoscience for lending us radioactive rocks, which enable us to conduct the radioactive experiment. At last, we appreciate Po-Yi Lin's help for lending us his power bank to conduct the experiments in the tunnels.

-
- [1] Jiwoo Nam (2023) *Instrumental Methods in Particle Astrophysics*, Lecture Slides.
 - [2] Auger, P., Ehrenfest, P., Maze, R., Daudin, J., & Fréon, R. A. (1939) *Extensive cosmic-ray showers*, Reviews of Modern Physics, 11(3-4), 288-291. doi:10.1103/revmodphys.11.288

- [3] Particle Detectors(2008) *Momentum measurement and Muon Detection*. 327-345. doi:10.1017/cbo9780511534966.014
- [4] Ltd., M. (1956). *Geiger tube*. *Journal of Scientific Instruments*, 33(8), 327-327. doi:10.1088/0950-7671/33/8/431

- [5] Rossi, B. (1930). *On the magnetic deflection of Cosmic Rays* Physical Review, 36(3), 606–606. doi:10.1103/physrev.36.606
- [6] Hess, V. (2018) *On the observations of the penetrating radiation during seven balloon flights* <https://arxiv.org/abs/1808.02927>.
- [7] Paolo Lipari(2000). *The east-west effect for atmospheric neutrinos* <https://arxiv.org/pdf/hep-ph/0003013.pdf>
- [8] Kampert, K.-H., & Watson, A. A. (2012). *Extensive air showers and ultra high-energy cosmic rays: A historical review* The European Physical Journal H, 37(3), 359–412. doi:10.1140/epjh/e2012-30013-x
- [9] Bonino, R., Alekseenko, V. V., Deligny, O., Ghia, P. L., Grigat, M., Letessier-Selvon, A., et al. (2011). *The east-west method: An exposure-independent method to search for large-scale anisotropies of Cosmic Rays*. The Astrophysical Journal, 738(1), 67. doi:10.1088/0004-637x/738/1/67
- [10] Sarkar, U. (2019). *Particle and Astroparticle Physics*. Boca Raton, FL: CRC Press.
- [11] KIMURA K(1940) *Study on radioactivity of Hukutolite in Taiwan by means of a counter with linear amplifier*
- [12] 陳, 培源; 劉, 德慶; 黃, 怡禎(2004). 臺灣之礦物. 經濟部中央地質調查所. pp. 125–133
- [13] Toptechboy Arduino lesson: Log sensor data to SD card
<https://toptechboy.com/arduino-lesson-21-log-sensor-data-to-an-sd-card/>